



# Functional mesoporous poly (ionic liquid) derived from P123: From synthesis to catalysis and alkylation of styrene and *o*-xylene

Beibei Wang | Xiaoli Sheng | Yuming Zhou | Zhiying Zhu | Yonghui Liu | Xiao Sha | Chao Zhang | Huaying Gao

School of Chemistry and Chemical Engineering, Southeast University, Jiangsu Optoelectronic Functional Materials and Engineering Laboratory, Nanjing 211189, People's Republic of China

## Correspondence

Xiaoli Sheng and Yuming Zhou, Huaying Gao School of Chemistry and Chemical Engineering, Southeast University, Jiangsu Optoelectronic Functional Materials and Engineering Laboratory, Nanjing 211189, People's Republic of China.  
Email: xlsheng@seu.edu.cn; ymzhou@seu.edu.cn

## Funding information

Priority Academic Program Development of Jiangsu Higher Education Institutions, Grant/Award Number: 1107047002; Fundamental Research Funds for the Central Universities, Grant/Award Numbers: 3207046409, 3207047402 and 2242015 k30001; Transformation of Scientific and Technological Achievements of Jiangsu Province of China, Grant/Award Number: BA2014100; Scientific Research Foundation of Graduate School of Southeast University, Grant/Award Numbers: YBJJ1731, YBJJ1733 and YBJJ1732; Graduate student scientific research innovation program of Jiangsu Province, Grant/Award Number: KYCX17\_0136 KYCX17\_0134; Qing Lan Project of Jiangsu Province, Grant/Award Number: 1107040167; Jiangsu Province of China, Grant/Award Number: JNHB-006; National Natural Science Foundation of China, Grant/Award Numbers: 51673040, 21376051 and 21676056

A novel strategy was proposed for the fabrication of high-performance acidic mesoporous poly ionic liquids catalyst. In this work, mesoporous poly ionic liquids (MPILs) were synthesized with P123 (PEO<sub>20</sub>PPO<sub>70</sub>PEO<sub>20</sub>) served as pore-forming agent. Then, MPILs were treated with PW<sup>3-</sup> anion exchange, thereby fabricating PW/MPIL-S(x). MPIL and PW/MPIL-S(x) were characterized by scanning electron microscope (SEM), transmission electron microscopy (TEM), Thermogravimetric analysis (TA), N<sub>2</sub> adsorption–desorption and Fourier transform infrared (FT-IR) spectra and X-ray photoelectron spectroscopy (XPS) spectra. The effect of solvent and concentration of P123 on the morphology and mesoporous structure of MPILs were investigated systematically. And the results show that MPILs were featured with mesoporous channel structure, high surface area (up to 737 m<sup>2</sup>/g) and large pore volumes (1.16 cm<sup>3</sup>/g), which benefit heterogeneous phase reaction (such as, alkylation of styrene with *o*-xylene). In the alkylation reaction, under optimal reaction conditions, the catalyst PW/MPIL-THF (4.0 g) shows high conversion of styrene (100%) and PXE yield (96.21%), demonstrating the excellent catalytic activities. Furthermore, PW/MPIL-S(x) are easy to be separated from the catalytic system by filtration and show no obvious decrease in catalytic activity after 6 cycle runs. The obtained PW/MPIL-S(x) catalyst exhibit high thermal and mechanical stability as well, indicating extensive application in high temperature acidic catalysis. This work might open up a new method for the synthesizing of porous polymer catalysts in the future.

## KEYWORDS

alkylation, catalyst, mesoporous poly ionic liquid, P123

## 1 | INTRODUCTION

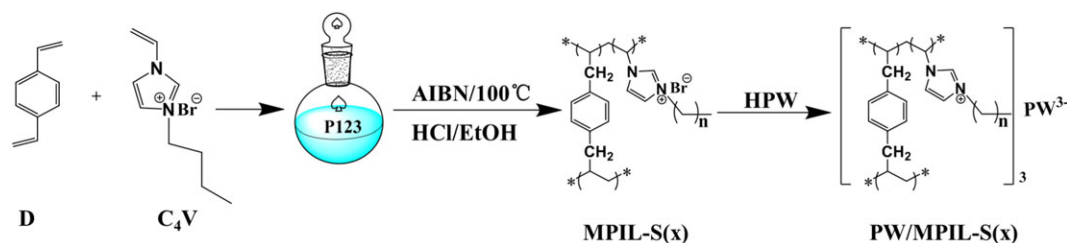
The Friedel-Crafts (F-C) reaction<sup>[1–3]</sup> is a key direct C-C bond forming reaction, which is one of the cornerstones of organic and industrial synthetic chemistry. For example, Phenylxylylene (PXE)<sup>[4]</sup> obtained by the alkylation of *o*-xylene with styrene has been widely used as excellent solvent. Generally, a strong acid catalyst such as H<sub>2</sub>SO<sub>4</sub>, AlCl<sub>3</sub> and Phosphotungstic acid (HPW) is essential to the F-C reaction. However, for traditional alkylation catalysts, there were series of disadvantages,<sup>[5]</sup> for instance, strong corrosivity, unstability, dangerous to handle and over-alkylation of the product, *etc.* Furthermore, the separation of catalysts from catalytic system is difficult. Facing to these problems, much efforts are still necessary to design and synthesize environmental catalysts with stable physicochemical properties and superior catalytic performance.

Recent research reveals that porous materials<sup>[6–9]</sup> are favorable carrier and catalyst due to their high surface area and much ordered channels. Porous materials (such as mesoporous silicon,<sup>[10]</sup> porous carbon,<sup>[11,12]</sup> macroporous polymers,<sup>[13]</sup> *etc.*) have a profound impact on heterogeneous catalysis.<sup>[14–16]</sup> For instance, Sai An *et al.* prepared a series of Arenesulfonic acid functionalized ethyl-bridged organosilica hollow nanospheres, ArSO<sub>3</sub>H-EtHNS, with different shell thicknesses (2–6 nm).<sup>[17]</sup> The ArSO<sub>3</sub>H-EtHNS has an excellent catalysis performance in the hydrolysis of furfuryl alcohol (FAL) to levulinic acid (LA). Christopher B. Smith *et al.* obtained Carbon-based solid acid catalyst from water hyacinth leaves by one-step hydrothermal carbonization, the presence of highest amount acid sites in the materials promote esterification of oleic acid and dehydration of xylose.<sup>[18]</sup> Previously, our research group conducted extensive research on solid acid catalysts, including zeolite supported Phosphotungstic acid and Zr doped sulfated mesoporous silica.<sup>[19–21]</sup> Nevertheless, some environmental problems and other drawbacks of these catalysts are still worth deeply pondering, the most serious problem is the losses of activity sites, which deriving from destruction of the channels structure.

Poly (ionic liquid) s (PILs) are an emerging class of functional polymers that are comprised of ionically charged repeating units typically used in ionic liquid

chemistry.<sup>[22–25]</sup> As a burgeoning interdisciplinary topic, PILs are attracting increasing interest due to the combination of the unique properties of IL with the macromolecular architecture and creating new properties and functions.<sup>[26–28]</sup> Recently, a series of PIL materials have been synthesized by introducing functional cationic and anionic IL groups into dynamic macromolecular polymeric architectures which have broadened PIL properties, structures, functionalities and applications.<sup>[29–32]</sup> PILs have been widely used in catalysis due to the function-designability and eco-friendly quality.<sup>[33–35]</sup> For example, Ali Pourjavadi and cooperators synthesized a dual acidic heterogeneous organocatalyst by copolymerization of acidic ionic liquid monomer ([VSim][HSO<sub>4</sub>]) and liquid crosslinker (1,4-butanediyl-3,3-bis-1-vinyl imidazolium dihydrogen sulfate).<sup>[36]</sup> The catalyst was shown to be an efficient dual acidic organocatalyst for Biginelli reaction under mild reaction conditions in high yields. Junke Wang *et al.* prepared a novel poly(4-vinylpyridine) supported acidic ionic liquid catalyst which acted as a heterogeneous catalyst to effectively catalyze the cyclocondensation reaction of anthranilamide with aldehydes under ultrasonic irradiation.<sup>[37]</sup> Except for the above studies, some researchers and scholars started to report porous PILs materials. That is to say, it's feasible to design and synthesize porous PILs which possess high surface areas and large pore volume. For instance, Zuowang Wu *et al.* prepared a Brønsted acidic PILs with Multi-layered macroporous structure which proved to be a novel and efficient heterogeneous acidic catalyst for biodiesel production.<sup>[38]</sup> Jing li and cooperators obtained a heteropolyanion-based acidic ionic liquid-functionalized mesoporous copolymer P (VB-VMS) PW (S<sub>BET</sub> = 191 m<sup>2</sup>/g), this catalyst shown superior acid catalysis performance in benzylation reaction.<sup>[39]</sup> Danuta Kuzmicz *et al.* acquired a series of mesoporous poly (ionic liquid) by solvothermal copolymerization of divinylbenzene and monomeric ionic liquids and the PILs which possessed excellent Physicochemical properties such as thermal stability, acid resistance and high surface areas.<sup>[40]</sup>

Herein, a novel strategy was proposed for the fabrication of high-performance acidic mesoporous poly ionic liquids catalyst. During the fabrication process, with P123



**FIGURE 1** Reaction scheme for the synthesis of catalyst PW/MPIL-S(x)

serve as soft template, mesoporous poly ionic liquids (MPILs) was synthesized via one step hydrothermal method. Followed by solvent extraction to remove P123. Later, the anion exchange property of the MPIL materials allows facile tuning of counter anions, through which the Keggin-structured phosphotungstic anion is exchanged and highly dispersed onto the surface of channels. The obtained PW/MPIL-S(x) exhibited perfect catalytic activities in alkylation of *o*-xylene and styrene because of high surface area and large pore volumes. Besides, the catalyst not only could be separated and recycled easily, but also shows high thermal and mechanical stability, thereby indicating the wide application fields in acidic catalysis. Figure 1 clearly shows reaction scheme for synthetic processes of catalyst.

## 2 | EXPERIMENTAL

### 2.1 | Materials

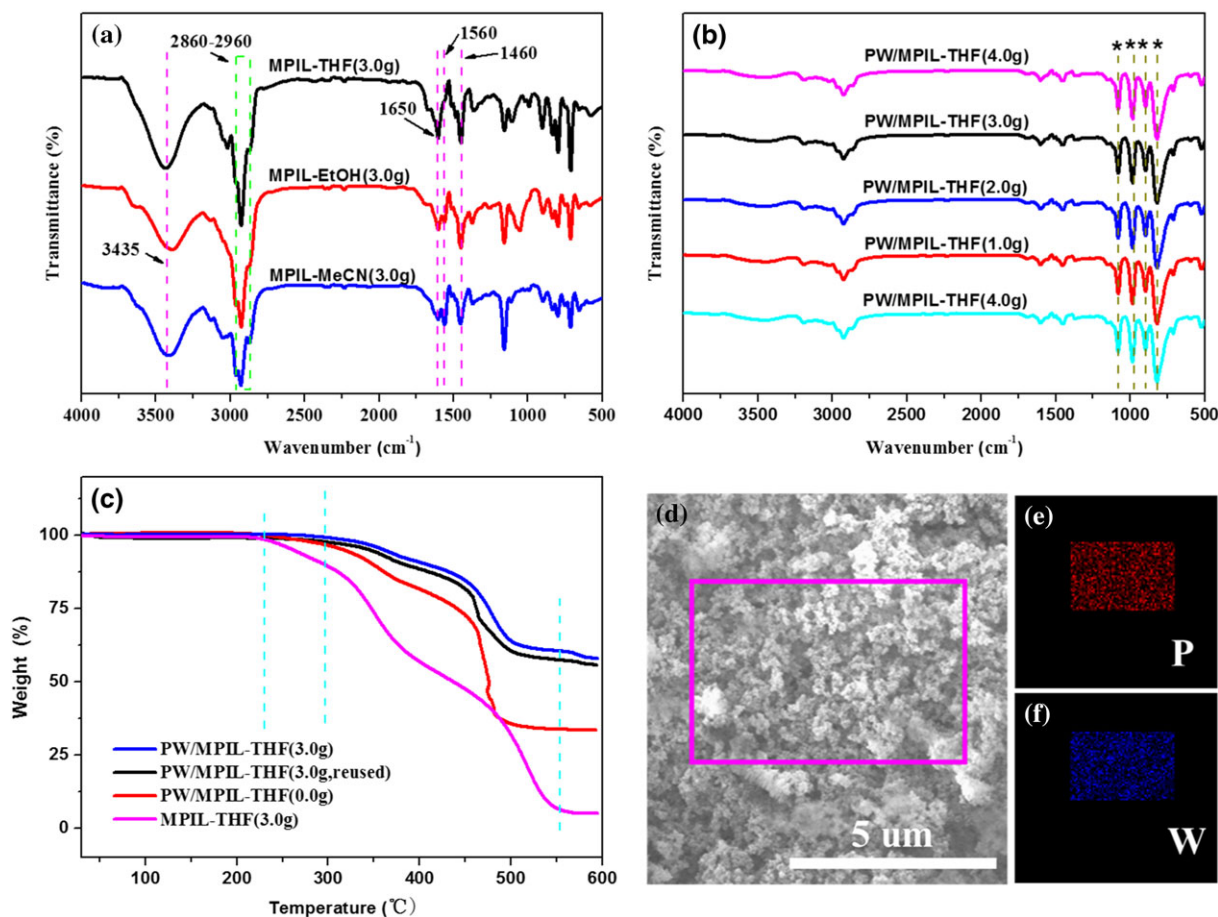
All chemicals were analytical grade and were used as received without further purification. P123 (PEO<sub>20</sub>PPO<sub>70</sub>PEO<sub>20</sub>) was purchased from Sigma-Aldrich.

Divinylbenzene (80.0%w) (D) and 1-butyl-3-vinylimidazolium bromide (99.0%w) (C<sub>4</sub>V) were used to synthesize poly ionic liquid which supplied by Energy chemical Co., Ltd. 2, 2'-Azobis (2-methylpropionitrile) (AIBN) were purchased from Aladdin Industrial Corporation. Phosphotungstic acid (HPW), acetonitrile (AR) (MeCN), tetrahydrofuran (AR) (THF) and ethanol absolute (AR) (EtOH) were purchased from Sinopharm Chemical Reagent Co., Ltd. Styrene and *o*-xylene were supplied by Shanghai Lingfeng Chemical Reagent Co., Ltd.

### 2.2 | Catalyst synthesis

#### 2.2.1 | Preparation of uniform size mesoporous poly ionic liquids materials

The uniform sized mesoporous poly ionic liquid (MPIL) were synthesized in analogy to a method described by Chenjue Gao et al.<sup>[41]</sup> The synthesis was achieved through free radical copolymerization of D with C<sub>4</sub>V in the presence of amphiphilic soft templates P123. In a typical reaction, 3.0 g P123 was dissolved using 30 ml THF. Subsequently, 2.31 g ionic liquid monomer C<sub>4</sub>V and



**FIGURE 2** FT-IR spectra (a-b) and TG curves (c) of samples, EDS elemental mapping analysis (d-f) of the catalyst PW/MPIL-THF(3.0g)

2.60 g DVB were added into above clear homogenous P123 solution with stirring more than 3 hr, in order to form well-dispersed micelles. Then 0.15 g AIBN was added to the mixture. After vigorous stirring 3 hours at room temperature, the mixture was transferred into 100 ml Teflon lined stainless steel autoclave for reacting at 100 °C for 24 hr. Then the white or yellowish solid was collected by filtration, washed with ethanol three times and dried under vacuum at 60 °C. Finally, the template was removed by extracting in HCl solution (150 ml ethanol and 1 ml concentrated aqueous HCl, 36–38%).

Similarly, a series of samples were synthesized by changing solvent or the amount of P123 during synthesis. The final products were named as MPIL-S(x), where S stands for the solvent and x means the amount of P123. As a comparison, samples without P123 were also prepared.

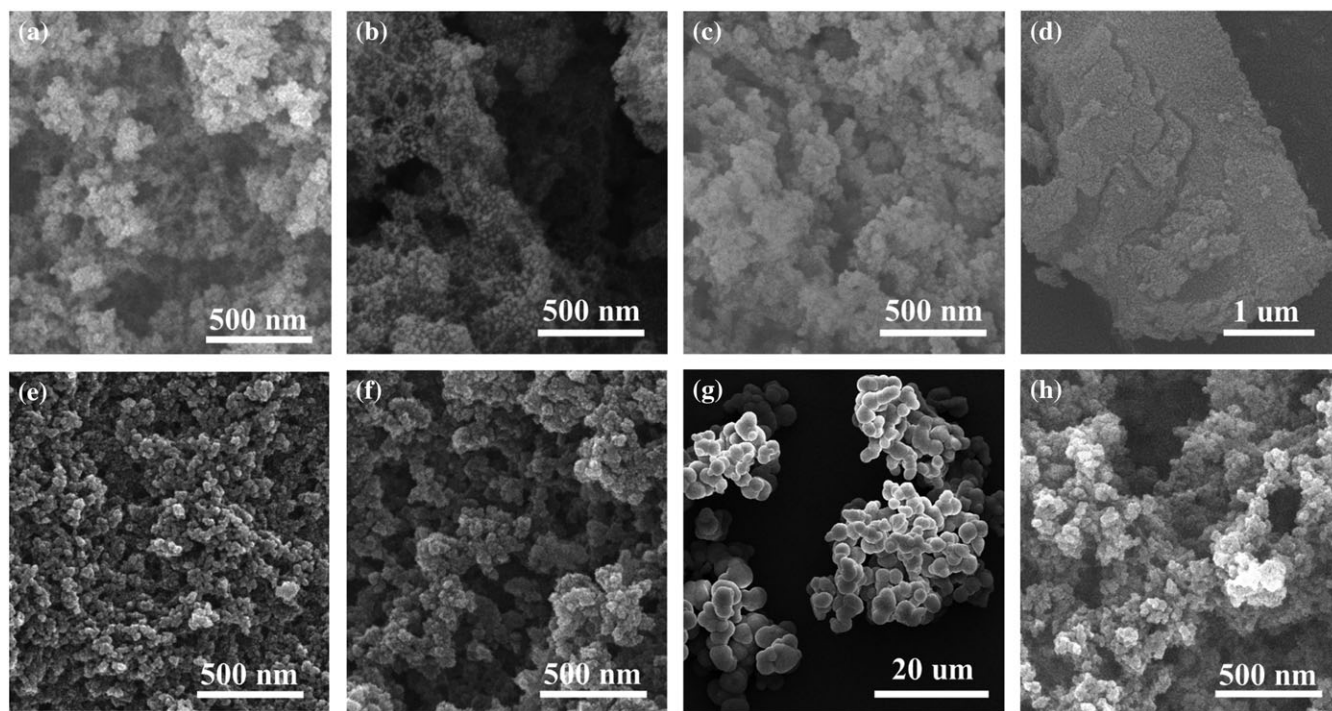
### 2.1.1 | Synthesis of acidic mesoporous poly ionic liquids (PW/MPIL-S(x))

Acidic mesoporous poly ionic liquids were prepared by impregnation according to the approach reported in the literature with a slight modification.<sup>[42]</sup> In a typical procedure, MPIL-S(x) (0.5 g) was added to 200 ml of the ethanol solution of 3.0 g HPW, and the mixture was

stirred at room temperature for 72 hr. Afterward, the white solid was collected by filtration and washed with ethanol for three times. After a vacuum drying at 60 °C for 24 hr, PW/MPIL-S(x) was obtained.

### 2.3 | Catalyst characterization

Scanning electron microscopy (SEM) images were recorded on a JEOL JSM-5600 L SEM instrument. Transmission Electron Microscopy (TEM) images were measured using FEI Tecnai G20 instrument. Specific surface areas and pore size distributions were carried out by Brunauer–Emmett–Teller (BET) method at –196 °C under an ASAP 2020 system, and the samples were outgassed in the degas port of the apparatus at 80 °C for 3 hr prior to testing. The pore size distribution in mesoporous range was analyzed by the BJH (Barrett–Joyner–Halenda) method. Fourier transform infrared (FT-IR) spectra were recorded on a BRUKER ALPHA FT-IR spectrometer. FT-IR spectrophotometer using anhydrous KBr as standard (1 wt% of the sample). Thermo Gravimetric Analysis (TGA) was performed using a Rigaku ThermoPlus TG8120 system at a rate of 10 °C min<sup>-1</sup> under air. The X-ray photoelectron spectroscopy (XPS) spectra were performed on a Thermo ESCALAB 250 with Al K $\alpha$  radiation.

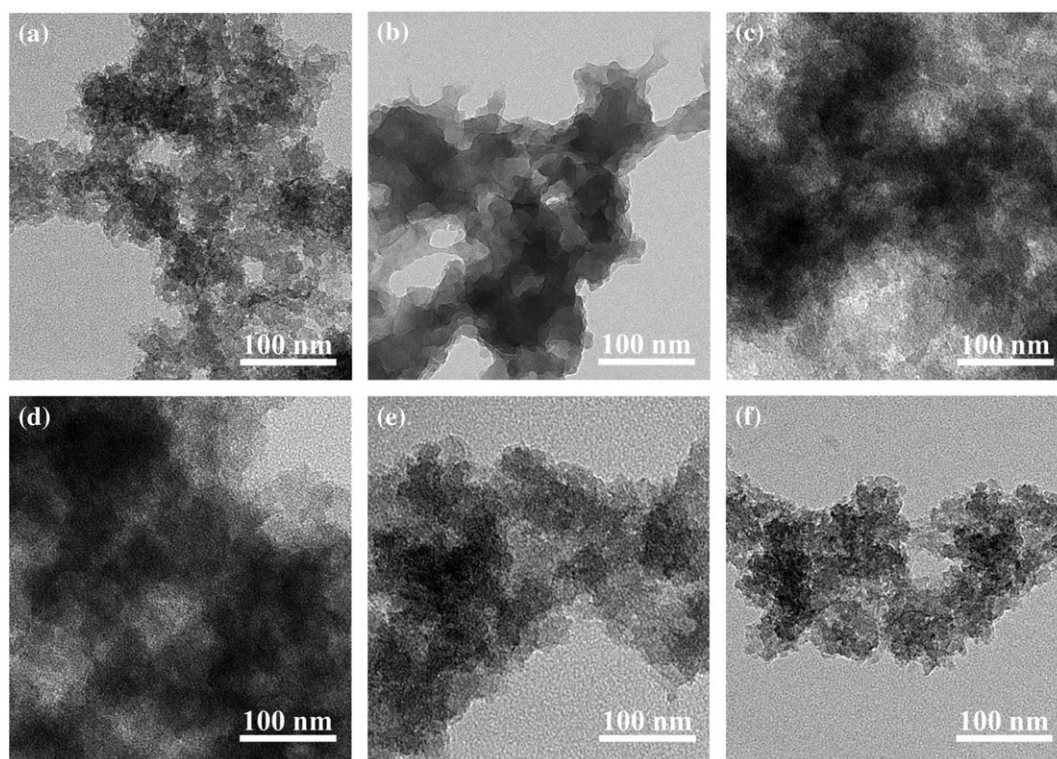


**FIGURE 3** SEM images of samples: (a) MPIL-THF(3.0g), (b) MPIL-EtOH(3.0g), (c) MPIL-MeCN(3.0g), (d) PW/MPIL-THF(0.0g), (e) PW/MPIL-THF(1.0g), (f) PW/MPIL-THF(2.0g), (g) PW/MPIL-THF(4.0g), (h) PW/MPIL-THF(3.0g)

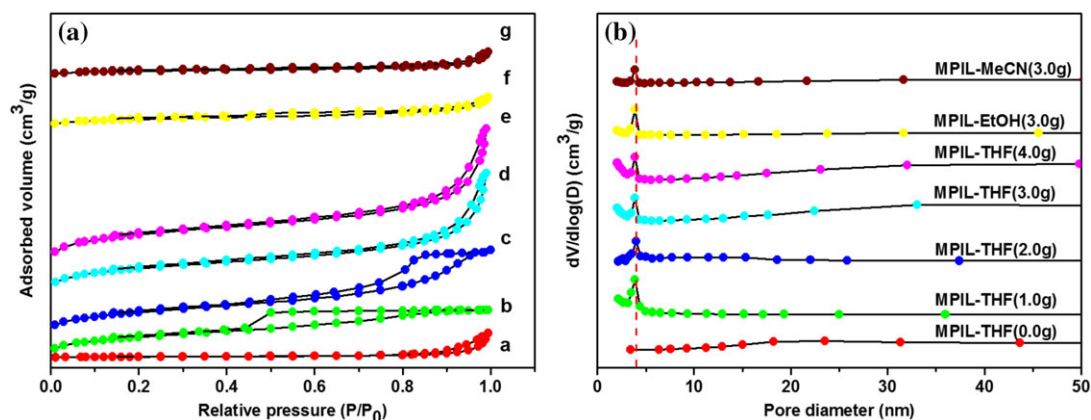
## 2.4 | Catalytic tests

The alkylation reactions were carried out in a continuously stirred batch reactor under reflux conditions using a three-neck 100 ml round-bottom flask equipped with a condenser. Preliminary runs were conducted with 4.0 g of styrene, 30.0 g of *o*-xylene (quality ratio of *o*-xylene to styrene, 7.5:1) and 0.25 g of catalyst at 120 °C for 180 min. At first, the 20.0 g *o*-xylene was initially added

to the reactor at the reaction temperature, followed by the desired amount of catalyst, the mixture of 4.0 g styrene and 10.0 g *o*-xylene was dripped slowly (about 2 hr) to the reaction mixture at the same temperature and continue to react for 1 hr. After the reaction, catalyst was recycled by vacuum filter and unreacted *o*-xylene was distilled out under atmospheric pressure, then a collected part was called as crude product. The crude product was analyzed with GC-9890A gas chromatograph equipped with OV-1



**FIGURE 4** TEM images of samples: (a) MPIL-THF(3.0g), (b) MPIL-EtOH(3.0g), (c) MPIL-MeCN(3.0g), (d) PW/MPIL-THF(0.0g), (e) PW/MPIL-THF(1.0g), (f) PW/MPIL-THF(3.0g)



**FIGURE 5** (a) N<sub>2</sub> adsorption-desorption isotherms of (a) MPIL-THF(0.0g), (b) MPIL-THF(1.0g), (c) MPIL- For Peer Review THF(2.0g), (d) MPIL-THF(3.0g), (e) MPIL-THF(4.0g), (f) MPIL-EtOH(3.0g) and (g) MPIL-MeCN(3.0g). (b) Pore size distribution calculated by BJH model based on desorption curves

capillary column and a flame ionization detector (FID). The yield of PXE was defined as follows:

$$\text{Yield of PXE (\%)} = \frac{\text{actual product weight}}{\text{theoretical product weight}} \times 100\% \quad (1)$$

$$\text{actual product weight} = \text{crude product weight} \times \text{PXE (chromatography)\%}$$

### 3 | RESULTS AND DISCUSSION

#### 3.1 | Catalyst characterization

As shown in the above FT-IR spectra (Figure 2 a-b), all samples exhibited a series of characteristic peaks, included  $3435\text{ cm}^{-1}$ ,  $1650\text{ cm}^{-1}$  and  $1560\text{ cm}^{-1}$ ,  $1460\text{ cm}^{-1}$  etc., which attributed to N-H stretching vibration, C=O stretching vibration and C=N stretching vibration of imidazole ring skeleton, imidazole ring C-H deformation vibration. Besides that, the observation of strong band at  $2860\text{--}2960\text{ cm}^{-1}$  were indicative of stretching vibrations of the C-H group. By observing FT-IR of MPIL which prepared in different solvents, no obvious difference was found. It can be seen clearly that the  $1082\text{ cm}^{-1}$  (P-O in the central tetrahedron),  $980\text{ cm}^{-1}$  (terminal W=O),  $896\text{ cm}^{-1}$  and  $812\text{ cm}^{-1}$  (W-O-W) in PW/MPIL-THF(x) from Figure 5 (b) which associated with Keggin ion.<sup>[43]</sup> This proved the Keggin structure of 12-tungstophosphoric acid was appeared after anion exchange with HPW. Energy-dispersive X-ray spectroscopy (EDS) elemental mapping analysis (Figure 2 (d-f)) to confirm the immobilization of PW species with a high dispersity which is consistent with FT-IR of PW/MPIL-THF(x).

Figure 2 (c) revealed the thermal stability of the samples. By comparing the image of TG curves, it can be find that all samples shown three thermal decomposition segments. At the first part, the decomposition maybe refer to solvent and physical adsorbed water (weight loss  $\leq 1\%$ ). Then the bond of copolymer of C<sub>4</sub>V and D start to rupture at  $300\text{ }^\circ\text{C}$ . Finally, the whole structure of MPIL was decomposed thoroughly about  $550\text{ }^\circ\text{C}$ . In last decomposition part, PW/MPIL-THF(x) were different from MPIL which appeared in MPIL almost completely degraded but PW/MPIL-THF(x) would not due to Keggin structure of 12-tungstophosphoric acid. What's more, PW/MPIL-THF (3.0 g) has higher stability than PW/MPIL-THF (0.0 g), and reused PW/MPIL-THF (3.0 g) (after 6 times) had a similar TG curves of fresh PW/MPIL-THF (3.0 g). The thermal stability of the catalyst can fully adapt to the alkylation.

The surface morphologies of the samples synthesized from different solvent or different P123 dosage were investigated by SEM (Figure 3). Almost all samples displayed a similar morphology of sphere-like aggregation. It can be clearly found the differences among the MPILs prepared in different solvents from Figure 3(a-c), among them, MPIL-THF (3.0 g) had more fluffy structure than the others. The dosage of P123 had a significant influence on morphology of PW/MPIL-THF(x). The shape of PW/MPIL-THF (0.0 g) was a monolith, on the contrary, the structure of catalyst had turn into sphere-like aggregation in the presence of P123, what's more, when the dosage of P123 increased to 4.0 g, the size of primary sphere-shaped particles up to 3–4  $\mu\text{m}$ .

The pore structure of the samples was further studied by TEM (Figure 4). By observing MPILs which prepared with different solvent from Figure 4 (a-c), the obvious mesoporous structure was discovered easily in MPIL-THF (3.0 g). Thus, a series of catalysts were synthesized which using tetrahydrofuran as a solvent with different amounts of P123. By comparing TEM images of PW/MPIL-THF(x) (Figure 4(d-f)), it's self-evident to confirmed that with the increase of the dosage of P123, the channel size became uniform. Meanwhile, the channel structure of PW/MPIL-THF (3.0 g) was consistent with MPIL-THF (3.0 g), it proved that MPILs kept high stability during the preparation process. Also, the exposure of active sites benefited from abundant mesoporous structure and eventually strengthened the catalytic activity.

The porosity of MPIL-S(x) is investigated by N<sub>2</sub> adsorption-desorption experiments. As displayed in Figure 5(a), all the samples exhibited the typical IV adsorption isotherms, which indicated the presence of mesoporous structures. Correspondingly, the pore size distribution (Figure 5(b)) was consistent with TEM. In addition to MPIL-THF (0.0 g), all samples shown only one peak at 4.5 nm which owed to the mesoscale micelles

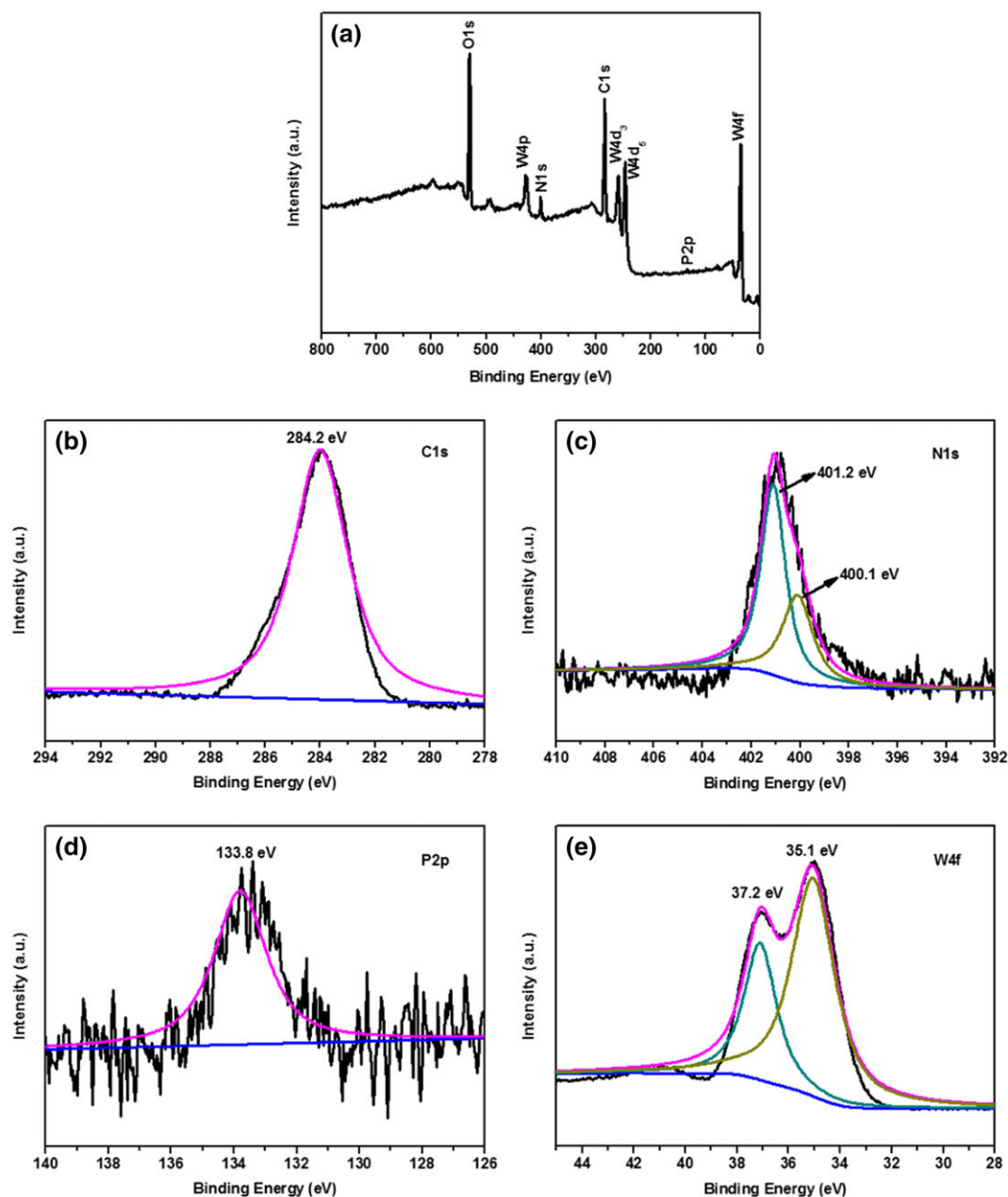
**TABLE 1** Physicochemical properties of the MPIL-S(x) which prepared at different condition

Sample Name	BET Surface Area ( $\text{m}^2/\text{g}$ )	Pore Volume ( $\text{cm}^3/\text{g}$ )	Average Pore Size (nm)
MPIL-THF(0.0 g)	37	0.22	29.01
MPIL-THF(1.0 g)	452	0.47	3.66
MPIL-THF(2.0 g)	513	0.77	5.94
MPIL-THF(3.0 g)	589	1.03	9.01
MPIL-THF(4.0 g)	737	1.16	8.67
MPIL-EtOH(3.0 g)	197	0.25	6.79
MPIL-MeCN(3.0 g)	97	0.19	10.43

of P123. Detailed physicochemical properties of samples listed in Table 1, MPIL-THF (3.0 g) possessed larger BET surface area ( $589 \text{ m}^2/\text{g}$ ) and pore volume ( $1.03 \text{ cm}^3/\text{g}$ ) than MPIL-EtOH (3.0 g) and MPIL-MeCN (3.0 g). This consequence caused by P123 aggregation behavior in different solvent. The dosage of P123 is vital to textural parameters of MPILs, it can be seen that with increasing P123 from 0.0 g to 4.0 g, the surface area of each sample is 37, 412, 513, 589 and  $737 \text{ m}^2/\text{g}$ , respectively, correspondingly, the pore volume of each sample is 0.22, 0.47, 0.77, 1.03 and  $1.16 \text{ cm}^3/\text{g}$ . To a great extent, the BET surface area and pore volume of MPILs enlarged with the increase of P123 content. In

short, possessing extremely large surface and pore volume of samples just like MPIL-THF (3.0 g) and MPIL-THF (4.0 g), which are beneficial to alkylation reaction of styrene and *o*-xylene.

XPS was performed to analyze the composition and valence states of the elements in the PW/MPIL-THF (3.0 g). The PW/MPIL-THF (3.0 g) was composed of C, N, O, P, W from the XPS wide scan spectrum (Figure 6a). The C1s spectrum shown a signal peak at about 284.2 eV, which was assigned to C-C bonds. The N1s spectrum can be deconvoluted into two peaks at 400.1 eV and 401.2 eV, corresponding to N-C and N=C bonds, respectively. The P2p spectrum displayed



**FIGURE 6** XPS wide scan spectra of PW/MPIL-THF(3.0g) (a) and C1s, N1s, P2p and W4f of PW/MPIL-THF(3.0g) (b-e)

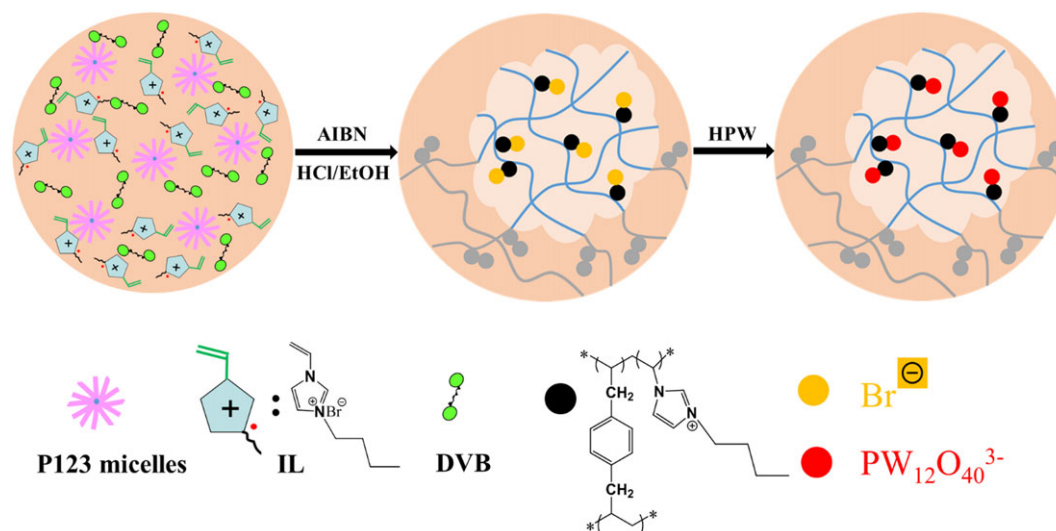
a wide signal peak at about 133.8 eV, ascribing the existence of  $P^{5+}$  in the oxidation state. Additionally, the W4f spectrum is deconvoluted into two significant peaks at 35.1 eV ( $4f_{5/2}$ ) and 37.2 eV ( $4f_{7/2}$ ), respectively, which are typically attributed to W in the W–O bond configuration and  $W^{6+}$  in HPW.<sup>[44]</sup> Combining XPS spectrum of P2p and W4f, it can be verify Keggin structure of 12-tungstophosphoric acid was loaded in the mesoporous channels successfully. The result was corresponding with Energy-dispersive X-ray spectroscopy elemental mapping analysis and FT-IR of PW/MPIL-THF (3.0 g).

Figure 7 reveals conjectural formation mechanism of PW/MPIL-s(x): as we all known, triblock P123 molecules can self-assemble into the mesoscale micelles in aqueous systems due to the hydrophobic core and the hydrophilic head group of amphiphilic molecules. On account of this, P123 plays an important role in the structure-directing aspect. During the synthesis of inorganic silicon materials, P123 usually is used as template because of the advantages of superior pore regulation effect. The polymerization process includes three parts. At first, forming a uniform transparent P123 micelle solution. The size of P123 micelles is different in different solution which affects pore size and pore size distribution of followed synthetic polymer. Then the dispersion process of ionic liquid monomers  $C_4V$  and cross-linker DVB is a critical intermediate process. Crosslinking polymerization process on micelle surface is the third section, in this stage, P123 micelles were wrapped by cross-linked polymerization products. Besides that, P123 micelles separated IL monomers which avoid IL homopolymerization or polymerization particles aggregation to bulk blocks. Only ionic liquid

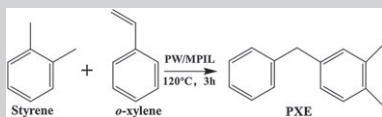
monomer  $C_4V$  and DVB fully disperse on the micelle surface, the third part polymerization process can take place on schedule. Subsequently, removing the template by solvent extraction and preparing catalyst PW/MPIL-S(x) by anion exchange. The difference of physicochemical properties of different samples maybe ascribe to P123 micelles distinction which caused by P123 aggregation behavior at different solvents and different dosages. Meanwhile, there is an interaction between P123 and IL monomer  $C_4V$  which mainly due to the hydrogen bond. So the interaction between P123 and  $C_4V$  is different with the increase of P123, when the dosage of P123 is low, the interaction between P123 and  $C_4V$  is weak. It's evident that the physicochemical properties of MPIL are affected by various factors. In general, the BET surface become lager with the increase of the dosage of P123 according to Table 1, at the same time, narrow pore size distribution is beneficial to catalytic reactions. Appropriate pores promote reactant molecules to contact with active sites and diffusion of products.

### 3.2 | Catalytic assessment

The Friedel-Crafts (FC) reaction is a key direct carbon-carbon bond forming reaction widely is used to prepare organic intermediates and employed for evaluating catalytic activity of the obtained mesoporous copolymeric solid acids. Table 2 listed the styrene conversion and PXE yield which using different catalyst precursor. According to the results, it can be clearly seen that HPW has excellent activities both yield (100%) and selectivity (100%) for this reaction, it's consistent with



**FIGURE 7** Hypothetical formation mechanism of PW/MPIL-S(x) catalyst

**TABLE 2** Yield of PXE and conversion of styrene in the alkylation of *o*-xylene and styrene


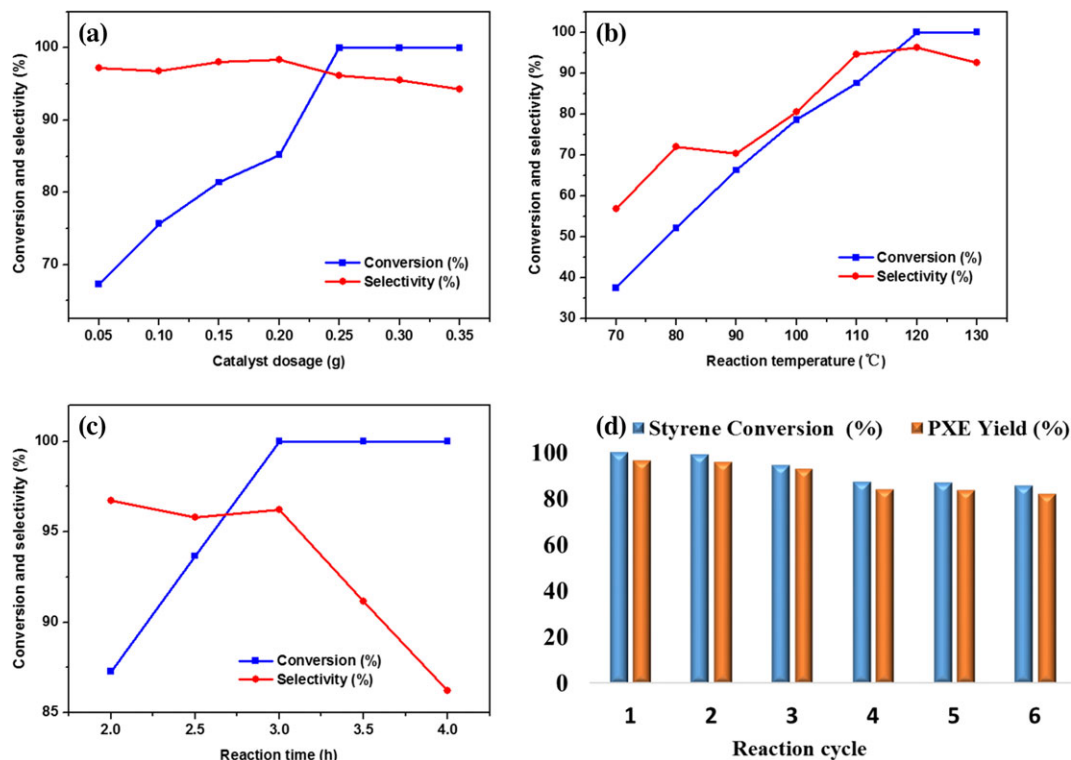
Catalyst	Styrene Conversion (%)	PXE Yield (%)
HPW	100	100
PW/MPIL-EtOH(3.0 g)	92.51	87.34
PW/MPIL-MeCN(3.0 g)	83.15	82.26
PW/MPIL-THF(4.0 g)	100	95.44
PW/MPIL-THF(3.0 g)	100	96.21
PW/MPIL-THF(2.0 g)	97.88	92.26
PW/MPIL-THF(1.0 g)	91.59	89.51
PW/MPIL-THF(0.0 g)	60.25	49.26

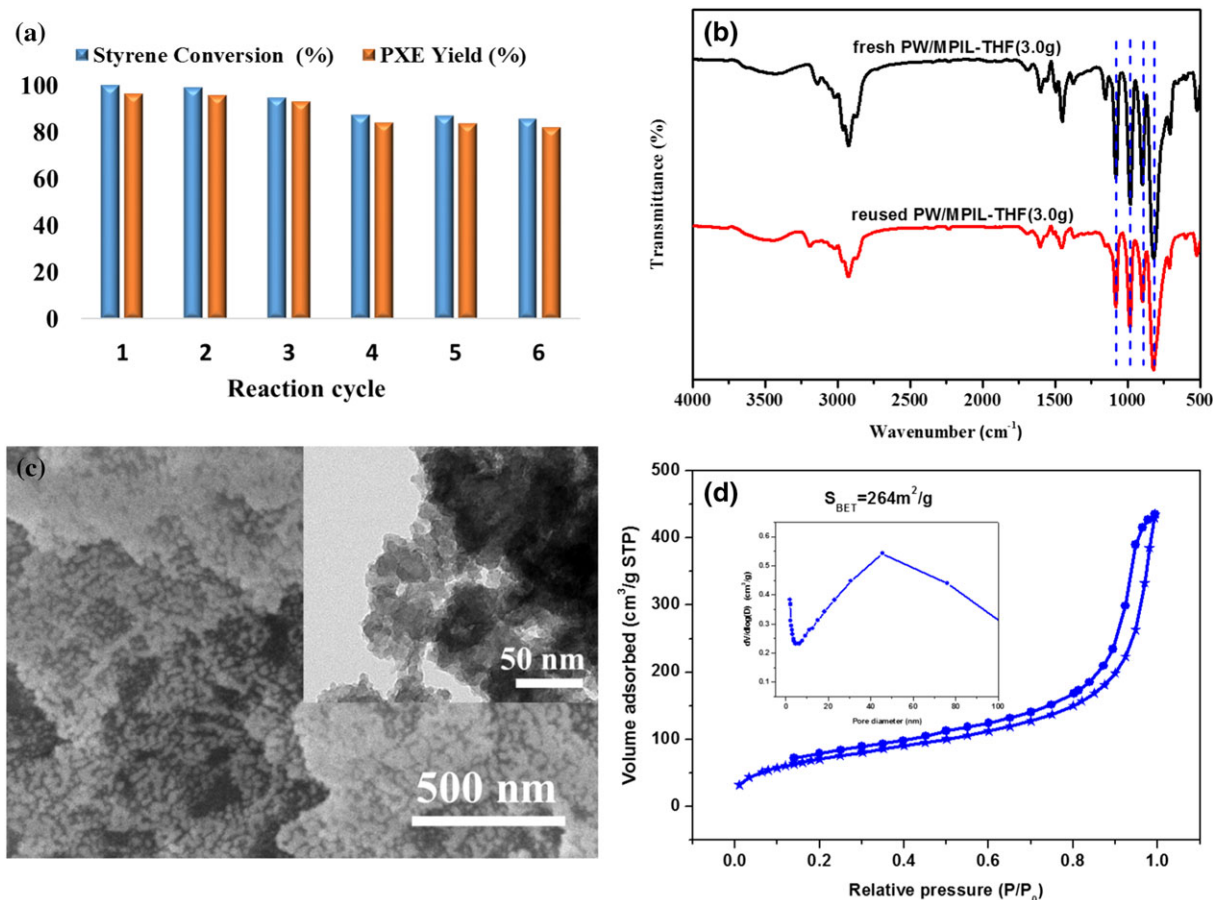
Sheng et al.<sup>[45]</sup> Nevertheless, it is difficult to purify production after reaction. At moment, the PW/MPIL-S(x) shows superiority which including abundant acid sites thanks to larger surface and pore volume, non-corrosive, environmentally friendly. What's more, compared with a

pure HPW, this catalyst was simply separated from mixture. As displayed in Table 2, it's obvious to find that all catalysts exhibit high PXE yield and good selectivity, indicating that PW/MPILs catalyst was prepared successfully via anion exchange with HPW. Among them, PW/MPIL-THF (3.0 g) and PW/MPIL-THF (4.0 g) exhibited the highest styrene conversion (100%). On the contrary, the catalyst activity of PW/MPIL-THF (0.0 g) was unsatisfactory with the styrene conversion and

PXE yield were 60.25% and 49.26%, respectively. By observing TEM image (Figure 3(d)) and BET (Figure 4 and Table 1), it can be find that the structure of MPIL-THF (0.0 g) was disadvantageous for the reaction, such as, low surface and pore volume. Therefore, the excellent catalytic performance of catalyst attributed to both the favorable structure and strong acid sites.

Additionally, the influence of reaction conditions was investigated systematically and displayed in Figure 8(a-b). Experiments were conducted under catalyst PW/MPIL-THF (3.0 g). The dosage of catalyst was verified as significant factor. According to Figure 8 (a), when the amount of catalyst from 0.05 g add up to 0.25 g, the conversion of styrene increase obviously. Whereas, when the dosage of catalyst from 0.25 g to 0.35 g, the selectivity decrease gradually. This consequence explained that overmuch

**FIGURE 8** Effect of the catalyst (PW/MPIL-THF(3.0g)) dosage (a), reaction temperature (b) and reaction time (c) on the conversion of styrene and selectivity of PXE. (Reaction condition: T=393 K, catalyst dosage=0.25 g, t=3.0 h). (d) Cycling performance test of PW/MPIL-THF (3.0g)



**FIGURE 9** Recycling of catalyst (PW/MPIL-THF(3.0g)) FT-IR spectrum of before reaction and after reaction(a), N<sub>2</sub> adsorption-desorption isotherms and pore size distribution (inset) of fresh catalyst and recovered catalyst (b), SEM image (c), TEM image (d)

catalyst is disadvantageous to reaction. For a defined catalytic system, too much catalyst will cause side reactions. Therefore, the appropriate amount of catalyst addition is important to the reaction. In this reaction, the optimal dosage of catalyst is 0.25 g (6.25% of styrene quality).

Figure 8(b) explored the effect of reaction temperature on the conversion of styrene and selectivity of PXE. Reaction temperature is another crucial factor to the catalyst reaction. The level of temperature determines whether the reaction can occur and the extent of side reactions. By analyzing the curves of conversion of styrene and selectivity of PXE in Figure 8 (b), it can be discovered easily that when the temperature was below 70 °C, the conversion of styrene was only 36.5%. With increasing of reaction temperature, the conversion of styrene increased significantly, the selectivity of PXE increased as the reaction temperature went up, in agreement with the conversion of styrene. What is noteworthy is that when the temperature exceed 120 °C, the selectivity of PXE start decreasing. When the reaction temperature exceed 120 °C, the side reactions maybe occur, such as polymerization of styrene, polysubstituted of benzene ring, etc. That is to say, 120 °C is the suitable reaction temperature

Reaction time also influences the conversion of styrene and selectivity of PXE. Figure 8 (c) expressed intuitively this result. When the process of reaction time from 2.0 hr to 4.0 hr, the conversion of styrene increased accordingly, later reached constant (100%) after 3 hr. On the contrary, the PXE selectivity trend curve was different with the conversion of styrene curve, the best selectivity obtained when reacted for 3 hr. In summary, the optimal reaction time is 3 hr.

### 3.3 | Catalyst recycling

Stability and reusability of the catalyst are crucial for any catalytic system. The cycling of the catalyst PW/MPIL-THF (3.0 g) has been tested via carrying out the reaction with used catalyst under the optimized conditions. The cycling results were summarized in Figure 8(d). It can be seen only 13% reduction in the activity is observed after 5 runs for the catalyst PW/MPIL-THF (3.0 g). The catalyst PW/MPIL-THF (3.0 g) was prepared by anion exchange, thus, it's difficult to loss the acid sites because of the strong interaction of the active composition and

support. And the PXE yield reached 84% after 5 times. Compared pure HPW, there was a little reduction of the conversion of styrene and PXE yield by using recovered catalyst, however, the PW/MPIL-THF(3.0 g) possessed untouchable advantage which including easily to separate and recycle than HPW.

In order to illustrate the structure and active site distribution of the recovered catalyst, a series of characterizations were carried out and the consequences which displayed in Figure 9. FT-IR spectra (Figure 9 (a)) exhibited similar characteristic peaks of fresh catalyst and recovered catalyst, confirming the presence of Phosphotungstic acid active component. From N<sub>2</sub> adsorption-desorption isotherms and pore size distribution (inset) of fresh catalyst and recovered catalyst, it can be observed that fresh catalyst possessed larger BET surface area (482 m<sup>2</sup>/g) than recovered catalyst (264 m<sup>2</sup>/g) which because of partial channels were destructed in the reaction. Pore size distribution insert Figure 9 (b) demonstrated the consistent pore size of fresh catalyst and recovered catalyst. Which shown mesoporous structure was preserved well after reaction and verified the high thermal and mechanical stability of PW/MPIL-THF (3.0 g). In addition, the SEM image and TEM image of recovered catalyst (Figure 9(c-d)) were similar to the fresh one, verifying a rather durable catalyst structure.

## 4 | CONCLUSION

In conclusion, a templating approach applied to successfully synthesize hierarchical mesoporous poly ionic liquid materials by using the soft template P123. The channel structure and physicochemical properties of MPIL-S(x) can be adjusted easily by choosing the suitable solvent and changing the dosage of P123. The MPILs materials can be easily modified chemically which ascribing to the special properties of the IL-like unit in the mesoporous polymer skeleton. So, synthesized heteropolyanion-loaded catalyst through exchanging with the acidic anions. The PW/MPIL-S(x) exhibited excellent catalytic activity in alkylation of styrene with *o*-xylene. Moreover, it could be easily recycled for industrially feasible compared to homogeneous catalysts.

## ACKNOWLEDGEMENTS

The authors are grateful to the financial supports of the National Natural Science Foundation of China (Grant No. 21676056, 21376051 and 51673040), "Six Talents Pinnacle Program" of Jiangsu Province of China (JNHB-006), Qing Lan Project of Jiangsu Province (1107040167), Graduate student scientific research innovation program of

Jiangsu Province (KYCX17\_0134 and KYCX17\_0136), Scientific Research Foundation of Graduate School of Southeast University (YBJJ1732, YBJJ1733, YBJJ1731), Fund Project for Transformation of Scientific and Technological Achievements of Jiangsu Province of China (Grant No. BA2014100), Fundamental Research Funds for the Central Universities (2242015 k30001, 3207047402, 3207046409) and A Project Funded by the Priority Academic Program Development of Jiangsu Higher Education Institutions (PAPD) (1107047002).

## ORCID

Beibei Wang  <https://orcid.org/0000-0001-6550-1074>

Chao Zhang  <https://orcid.org/0000-0002-0143-9504>

## REFERENCES

- [1] T. P. Maloney, K. L. Murphy, T. L. Mainsah, K. A. Nolin, *Tetrahedron Lett.* **2018**, *59*, 18.
- [2] Y.-Y. Ding, D.-F. Xu, S.-S. Meng, Y. Li, J.-L. Zhao, *Adv. Synth. Catal.* **2018**, *360*, 664.
- [3] S. Singhal, S. Agarwal, S. Arora, N. Singhal, A. Kumar, *Catal. Sci. Technol.* **2017**, *7*, 5810.
- [4] H. Gao, Y. Zhou, X. Sheng, S. Zhao, C. Zhang, J. Fang, B. Wang, *Appl. Catal. A-Gen.* **2018**, *552*, 138.
- [5] X. Fu, X. Sheng, Y. Zhou, Z. Fu, S. Zhao, X. Bu, C. Zhang, *RSC Adv.* **2016**, *6*, 50630.
- [6] B. Coasne, A. Galarneau, R. J. Pellenq, F. Di Renzo, *Chem. Soc. Rev.* **2013**, *42*, 4141.
- [7] S. Chen, P. Li, S. Xu, X. Pan, Q. Fu, X. Bao, *J. Mater. Chem. A* **2018**, *6*, 1832.
- [8] X.-H. Li, Y.-W. Liu, S.-M. Liu, S. Wang, L. Xu, Z. Zhang, F. Luo, Y. Lu, S.-X. Liu, *J. Mater. Chem. A* **2018**, *6*, 4678.
- [9] E. Yang, E. J. Jang, J. G. Lee, S. Yoon, J. Lee, N. Musselwhite, G. A. Somorjai, J. H. Kwak, K. An, *Catal. Sci. Technol.* **2018**.
- [10] M. Hartmann, A. G. Machoke, W. Schwieger, *Chem. Soc. Rev.* **2016**, *45*, 3313.
- [11] Y. Xia, Z. Yang, Y. Zhu, *J. Mater. Chem. A* **2013**, *1*, 9365.
- [12] S. Liu, Y. Liang, W. Zhou, W. Hu, H. Dong, M. Zheng, H. Hu, B. Lei, Y. Xiao, Y. Liu, *J. Mater. Chem. A* **2018**, *6*, 12046.
- [13] J. Yin, G. Yang, H. Wang, Y. Chen, *Chem. Commun.* **2007**, 4614.
- [14] S. S. Chen, T. Maneerung, D. C. W. Tsang, Y. S. Ok, C.-H. Wang, *Chem. Eng. J.* **2017**, *328*, 246.
- [15] Y. Wang, D. Zhao, L. Wang, X. Wang, L. Li, Z. Xing, N. Ji, S. Liu, H. Ding, *Fuel* **2018**, *216*, 364.
- [16] M. Ran, J. Li, W. Cui, Y. Li, P. Li, F. Dong, *Catal. Sci. Technol.* **2018**.
- [17] S. An, D. Song, Y. Sun, Q. Zhang, P. Zhang, Y. Guo, *ACS Sustainable Chem. Eng.* **2018**, *6*, 3113.
- [18] J. Lao, C. B. Smith, S. M. Smith, *Chem. – Asian J.* **2017**, *12*, 3178.
- [19] S. Zhao, X. Sheng, Y. Zhou, M. He, X. Fu, Y. Zhang, *J. Porous Mater.* **2015**, *22*, 1407.

- [20] S. Zhao, M. He, Y. Zhou, X. Sheng, X. Fu, Y. Zhang, *RSC Adv.* **2015**, *5*, 28124.
- [21] M. Zhang, X. Sheng, Y. Zhang, Y. Zhou, S. Zhao, X. Fu, H. Zhang, *J. Porous Mater.* **2016**, *24*, 109.
- [22] W. Zhang, C. Willa, J.-K. Sun, R. Guterman, A. Taubert, J. Yuan, *Polymer* **2017**, *124*, 246.
- [23] M. R. Gao, J. Yuan, M. Antonietti, *Chemistry* **2017**, *23*, 5391.
- [24] H. He, D. Luebke, H. Nulwala, K. Matyjaszewski, *Macromolecules* **2014**, *47*, 6601.
- [25] A. J. Erwin, W. Xu, H. He, K. Matyjaszewski, V. V. Tsukruk, *Langmuir* **2017**, *33*, 3187.
- [26] Z. Xue, L. Qin, J. Jiang, T. Mu, G. Gao, *Phys. Chem. Chem. Phys.* **2018**, *20*, 8382.
- [27] J. Yuan, D. Mecerreyes, M. Antonietti, *Prog. Polym. Sci.* **2013**, *38*, 1009.
- [28] J. Yuan, M. Antonietti, *Polymer* **2011**, *52*, 1469.
- [29] W. Qian, J. Texter, F. Yan, *Chem. Soc. Rev.* **2017**, *46*, 1124.
- [30] S. Hayano, K. Ota, H. T. Ban, *Polym. Chem.* **2018**, *9*, 948.
- [31] T. Zhou, X. Gao, B. Dong, N. Sun, L. Zheng, *J. Mater. Chem. A* **2016**, *4*, 1112.
- [32] A. Dani, K. Tauber, W. Zhang, H. Schlaad, J. Yuan, *Macromol. Rapid Commun.* **2017**, *38*, 1700167.
- [33] Y. Zhang, Y. Zhang, B. Chen, L. Qin, G. Gao, *ChemistrySelect* **2017**, *2*, 9443.
- [34] Z. Guo, Q. Jiang, Y. Shi, J. Li, X. Yang, W. Hou, Y. Zhou, J. Wang, *ACS Catal.* **2017**, *7*, 6770.
- [35] H. Wang, X. Meng, G. Zhao, S. Zhang, *Green Chem.* **2017**, *19*, 1462.
- [36] A. Pourjavadi, S. H. Hosseini, R. Soleyman, *J. Mol. Catal. A-Chem.* **2012**, *365*, 55.
- [37] J. Wang, Y. Zong, R. Fu, Y. Niu, G. Yue, Z. Quan, X. Wang, Y. Pan, *Ultrason. Sonochem.* **2014**, *21*, 29.
- [38] Z. Wu, C. Chen, Q. Guo, B. Li, Y. Que, L. Wang, H. Wan, G. Guan, *Fuel* **2016**, *184*, 128.
- [39] J. Li, Y. Zhou, D. Mao, G. Chen, X. Wang, X. Yang, M. Wang, L. Peng, J. Wang, *Chem. Eng. J.* **2014**, *254*, 54.
- [40] D. Kuzmicz, P. Coupillaud, Y. Men, J. Vignolle, G. Vendramineto, M. Ambrogi, D. Taton, J. Yuan, *Polymer* **2014**, *55*, 3423.
- [41] C. Gao, G. Chen, X. Wang, J. Li, Y. Zhou, J. Wang, *Chem. Commun.* **2015**, *51*, 4969.
- [42] Y. Shi, Z. Guo, Q. Wang, L. Zhang, J. Li, Y. Zhou, J. Wang, *ChemCatChem* **2017**, *9*, 4426.
- [43] Y.-L. Peng, J. Liu, H.-F. Zhang, D. Luo, D. Li, *Inorg. Chem. Fron.* **2018**.
- [44] H. Wang, C. Wang, Y. Yang, M. Zhao, Y. Wang, *Catal. Sci. Technol.* **2017**, *7*, 405.
- [45] X. Sheng, J. Kong, Y. Zhou, Y. Zhang, Z. Zhang, S. Zhou, *Micropor. Mesopor. Mater.* **2014**, *187*, 7.

**How to cite this article:** Wang B, Sheng X, Zhou Y, et al. Functional mesoporous poly (ionic liquid) derived from P123: From synthesis to catalysis and alkylation of styrene and *o*-xylene. *Appl Organometal Chem.* 2019;e4719. <https://doi.org/10.1002/aoc.4719>